Slow wave propagation and sheath interaction in the ion-cyclotron frequency range

J. R. Myra and D. A. D'Ippolito

Lodestar Research Corporation, Boulder, Colorado

Aug 2009

submitted to *Plasma Physics and Controlled Fusion*

DOE/ER/54392-53 & DOE/ER/54823-7 LRC-09-129

LODESTAR RESEARCH CORPORATION

2400 Central Avenue

Boulder, Colorado 80301

Slow wave propagation and sheath interaction in the ion-cyclotron frequency range

J R Myra and D A D'Ippolito

Lodestar Research Corp., 2400 Central Ave. P-5, Boulder, Colorado 80301

Abstract. In previous work [Myra J R and D'Ippolito D A 2008 *Phys. Rev. Lett.* **101** 195004] we studied the propagation of slow-wave resonance cones launched parasitically by a fast-wave antenna into a tenuous magnetized plasma. Here we extend the treatment of slow wave propagation and sheath interaction to "dense" scrape-off-layer plasmas where the usual cold-plasma slow wave is evanescent. Using the sheath boundary condition, it is shown that for sufficiently close limiters, the slow wave couples to a sheath plasma wave and is no longer evanescent, but radially propagating. A self-consistent calculation of the rf-sheath width yields the resulting sheath voltage in terms of the amplitude of the launched slow wave, plasma parameters and connection length. The conditions for avoiding potentially deleterious rf-wall interactions in tokamak rf heating experiments are summarized.

PACS: 52.35.Mw, 52.40.Kh, 52.50.Qt, 52.55.Fa

I. Introduction

Ion-cyclotron-range of frequencies (ICRF) waves provide a reliable and versatile method of auxiliary heating in tokamaks, and are also of interest for other applications including current drive, and possibly flow drive. However, in some situations, it is observed experimentally that ICRF waves can interact in an unfavorable way with the walls and limiters of the device [1] causing enhanced sputtering, impurity generation, and parasitic power loss. ICRF sheath interactions on the conducting surfaces of the antenna, limiters and walls of the machine can be responsible for these phenomena, as reviewed in Refs. [1] and [2]. Detrimental effects have usually been minimized or avoided in present day experiments by a combination of careful antenna design, control of the launched rf power spectrum, and the conditions in the scrape-off-layer (SOL). However, an improved theory and modeling capability is needed to aid in the design of hardware and to clarify the plasma and rf conditions where successful operation can be expected. Furthermore, as fusion research progresses from short pulse experiments towards steady-state high-grade plasmas in ITER, [3] the limitations on acceptable rf sheaths and rf power deposition on plasma-facing components in the SOL will be more severe.

The basic physical mechanism for rf sheaths is well known, [4] although the details depend on the wave and plasma regime. Essentially, the lighter mass and stronger response of electrons to rf $E_{||}$ fields (parallel to the background magnetic field **B**) near surfaces leads to the development of rf-enhanced dc sheath potentials to confine the electrons and maintain quasineutrality. (See e.g. Ref. 2 and refs therein.) Since the magnetosonic fast wave (FW) has a negligible $E_{||}$, ICRF-generated sheaths are naturally associated with the slow wave (SW). Ideally if a wave with pure FW polarization could be launched and maintained throughout the entire volume, sheath formation would not be an issue. However, in practice this is not possible, and it has been recognized for a long time that parasitic SW generation is likely responsible for the high voltage sheaths observed in experiments.[5-11]

This paper is one of a series of papers in which we explore the role of an rf sheath boundary condition [12-15] on SW generation, propagation and wall interaction. To place the present paper in context with respect to earlier studies, we first consider several mechanisms by which the SW can arise near material boundaries.

The first mechanism involves conversion of the FW to the SW. In some situations the FW can access the wall, e.g. due to SOL propagation [16] or poor central absorption. [17-19] It was shown [12,20] that when flux surfaces do not match the wall shape, the boundary conditions (BCs) require generation of the SW. Specifically, the SW is generated when the background

magnetic field has a component into a conducting surface. In that situation the FW polarization (perpendicular to **B**) is in conflict with the requirement that the tangential electric field vanishes in the conductor. In Ref. 20 we considered a "scattering" problem, where an incoming FW reflected off of a self-consistent rf wall sheath, giving rise to a reflected FW and a SW.

On the antenna, rf $E_{||}$ fields can be generated directly by the current straps, which are usually vertical and therefore not exactly perpendicular to **B** because of the field line pitch. This direct driving of a near field $E_{||}$ causes sheaths on the antenna structure which were examined in Refs. [21] and [22] in a "waveguide" geometry meant to model the antenna box itself. Much more realistic antenna models including a detailed representation of the three-dimensional structure of the antenna have been developed and employed to obtain vacuum field solutions of Maxwell's equations for antenna modeling. [23,24] The incorporation of plasma effects and sheath boundary conditions into these models is a topic of current research. [25] In some cases, $E_{||}$ fields induced by the feeders and/or antenna box structure are also important, and even dominant over those generated directly by the current straps. [26]

As illustrated in Fig. 1, the presence of $E_{||}$ near the plasma-facing surfaces of the antenna structure, whatever the mechanism, also provides a source for SWs that can then propagate or evanesce into the SOL. The characteristics of the SW imply propagation approximately along the magnetic field. A mechanism of this type is likely to be involved in explaining observations on Alcator C-Mod [27] which link the rf-sheath location on remote limiters along field lines to the antenna. [28,29]

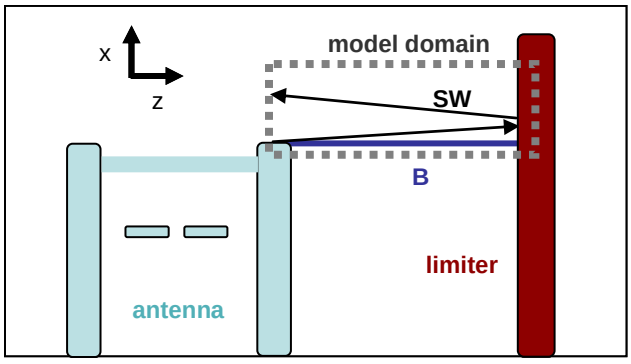

Fig. 1 Schematic of FW antenna looking down on the torus. SWs and sheaths present at the plasma-facing surfaces act as sources for SW propagation into the SOL where interaction with other surfaces can occur. The dashed region is half of the (assumed symmetric) domain of the model for this paper.

To describe this situation, we consider a model problem whose context is illustrated in Fig. 1. The dashed region is half of the (assumed symmetric) domain of the model for this paper, in which we consider the "aperture" problem for SW propagation and sheath interaction in the SOL. SWs are emitted from a localized source into a box bounded by conducting (and hence sheath-bearing) surfaces. We study the spreading, evanescence and propagation of these waves.

The purpose of the model is to gain conceptual insight into the underlying physics, therefore we restrict our attention here to simple rectangular geometries with a constant density SOL. For analysis and predictive capability useful for quantitative design studies and experimental modeling, a much more sophisticated model is clearly required. A numerical solution of wave propagation and sheath interaction with the SOL and plasma boundaries with more realistic geometry and plasma profiles is also in progress. [30]

In a recent work [31] we studied the propagation of SW resonance cones into a tenuous magnetized plasma, $\omega > \omega_{lh}$. Here ω_{lh} is the lower-hybrid frequency defined by

$$\omega_{lh}^2 = \Omega_i^2 + \omega_{pi}^2 \tag{1}$$

where $\Omega_i = ZeB/m_i c$ and $\omega_{pi}^2 = 4\pi n Z^2 e^2 / m_i$ define the ion cyclotron and ion plasma frequencies respectively. When $\omega > \omega_{lh}$, the SW propagates because the perpendicular plasma dielectric satisfies the inequality $\varepsilon_\perp > 0$. In the electrostatic limit, the SW propagation occurs in

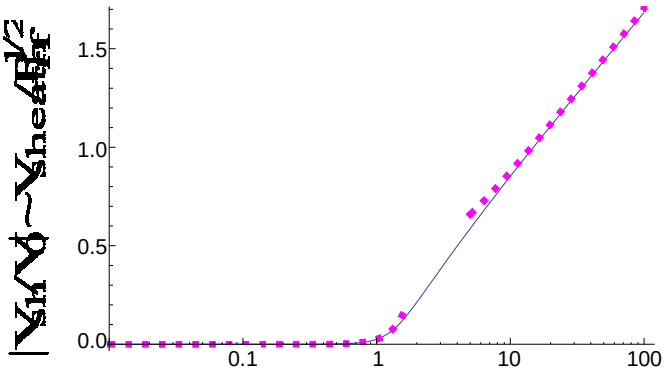

Fig. 2 The limiter sheath voltage V_{sh} as a fraction of the voltage V_0 launched into the resonance cone vs. an rf sheath parameter Λ_0. Here $a_{||}$ is the parallel scale length of the resonance cone structure, P_{rf} is the rf power and n_e is the plasma density. Dots are analytic asymptotic results described in Ref. 31. [Adapted from Ref. 31.]

resonance cones. The resonance cones interact with, and reflect from, the plasma sheath near a conducting wall. A key result from that study is reproduced in Fig. 2, for later comparison with the present calculation. Fig. 2 illustrates that the fraction of launched voltage in the resonance cones that is transmitted to the sheath has a sensitive threshold-like turn-on, which controls the onset of strong and potentially deleterious rf-wall interactions in a tokamak. The threshold depends primarily on the rf power and the plasma density.

In the present paper, we extend this investigation to "dense" SOL plasmas, $\omega < \omega_{lh}$, where the usual cold-plasma SW is evanescent, but here we will see that the SW can still propagate. As in Ref. 31, the key question here is how much of the rf sheath voltage at the antenna source appears across limiter sheaths in the SOL, and how this depends on the field line length and the rf source strength. Our paper is an expanded version of results that were briefly summarized in a recent conference proceedings. [32]

II. Wave propagation model

For the constant density plasma case in rectangular geometry that we consider in this paper, a simple method of solution of the aperture problem is eigenfunction expansion. The model geometry is given in Fig. 3. The equilibrium magnetic field **B** is along z, x is radial (increasing towards the plasma core) and y is ignorable. Let $\psi_m(x, z)$ for m = 0, 1, 2, … be eigenfunctions of the box which satisfy the SW dispersion relation in the plasma volume, and the sheath BCs at the wall (which will be introduced explicitly later). Then the source function for $E_{||}(z)$ specified at x = 0 is expanded as

$$S(z) = \sum_m C_m \psi_m(0,z) \tag{2}$$

and the solution throughout the volume is

$$E_z(x,z) = \sum_m C_m \psi_m(x,z) \tag{3}$$

Determining the eigenfunctions of the box subject to sheath BCs in z and outgoing/evanescent BCs in x is the first step. This problem was treated in Ref. 13 for the electrostatic odd parity modes. Here we need the even parity modes (and retain electromagnetic terms), but the methodology is the same, as will be recapitulated briefly in the next subsection.

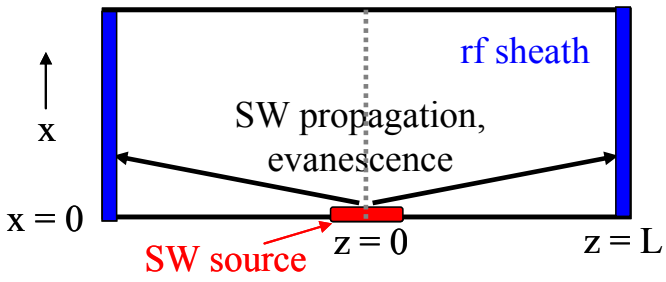

Fig. 3 Geometry of the model problem. The magnetic field is along z and x is the radial direction, increasing towards the core plasma. We consider even parity modes in $E_{||}(z)$ in a symmetric domain.

A. Eigenfunctions

In the plasma volume we look for eigenfunctions of the form $\psi_m \sim \cos(k_z z)\exp(ik_x x)$. The local SW dispersion relation is taken as

$$n_x^2 = \frac{\varepsilon_{||}}{\varepsilon_\perp}(\varepsilon_\perp - n_z^2) \tag{4}$$

where the usual cold fluid dielectric constants are employed:

$$\varepsilon_{||} = 1 - \frac{\omega_{pe}^2}{\omega^2} \tag{5}$$

$$\varepsilon_\perp = 1 - \frac{\omega_{pi}^2}{\omega^2 - \Omega_i^2} \tag{6}$$

and $\mathbf{n} = \mathbf{k}c/\omega$ with wavenumber $\mathbf{k} = k_x\mathbf{e}_x + k_z\mathbf{e}_z$. In the "dense" plasma limit considered in this paper, both $\varepsilon_{||}$ and $\varepsilon_\perp$ are negative. At the wall, z = L, we invoke the sheath BC [12,13]

$$E_x = -ik_x \Delta \varepsilon_{||} E_z \tag{7}$$

Here Δ is the width of the rf-sheath (modeled as a thin vacuum layer). The sheath BC is obtained by continuity of the normal (to the surface) component of $\mathbf{D} = \varepsilon\cdot\mathbf{E}$ and the tangential component of $\mathbf{E}$ across the sheath plasma interface.

The SW eigenvector for modes even in $E_z(z)$ is (see Appendix A)

$$\mathbf{E} = -i\frac{n_x n_z}{\varepsilon_\perp - n_z^2}\sin(k_z z)\mathbf{e}_x + \cos(k_z z)\mathbf{e}_z \tag{8}$$

The global dispersion relation, which gives the SW eigenfunctions of the box accounting for sheath BCs, is obtained by substituting E_x and E_z from Eq. (8) into Eq. (7),

$$\eta \tan \eta = (\eta^2 + b^2)\Lambda \tag{9}$$

where $\eta = k_z L$, $\eta_0 = \omega L / c$ and

$$b^2 = -\varepsilon_\perp \eta_0^2 > 0 \tag{10}$$

$$\Lambda = -\frac{\Delta\varepsilon_\parallel}{L} \tag{11}$$

In terms of these parameters the local dispersion relation Eq. (4) determining k_x is

$$k_x^2 \delta_e^2 = -\left(1 + \frac{\eta^2}{b^2}\right) \tag{12}$$

The fundamental sheath parameter is Λ. In the limiting case $\Lambda = 0$ we recover metal wall boundary conditions ($E_x = 0$) and in the opposite limit $\Lambda = \infty$ the surface acts like a perfect insulator ($E_z = 0$). The parameter b describes electromagnetic effects; $b = 0$ is the electrostatic limit. From Eq. (10) for $\omega >> \Omega_i$ and high densities ($\omega << \omega_{pi}$) we have the approximate scaling $b \sim L/\delta_i$ where δ_i is the ion skin depth.

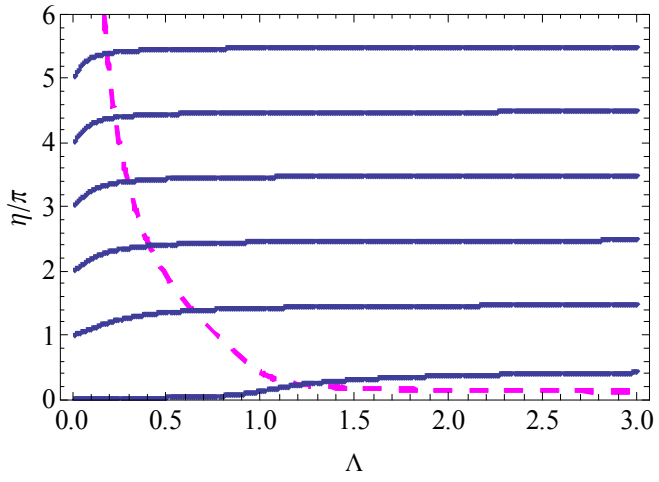

Fig. 4 Roots of the global dispersion relation Eq. (9) vs. sheath parameter Λ for the case $b = 0.1$. Real η roots (solid), Im η root, the SPW, (dashed).

The roots of Eq. (9) are shown in Fig. 4 for the case b = 0.1. For the metal wall limit $\Lambda = 0$ the roots are at $\eta_m = m\pi$ (m = 0, 1, 2, …). In the opposite (insulating wall) limit $\Lambda = \infty$ the roots are at $\eta_m = m\pi/2$ (m = 1, 3, 5 …). For intermediate Λ the roots transition between these cases, but there is also a new root with purely imaginary η.

This new root is the sheath-plasma wave (SPW). [20,33-35] Eigenfunctions of the SPW are localized in z to the sheaths for $\Lambda << 1$ (since from Fig. 4, Im $\eta >> 1$), and have the character of surface waves that exist because of the plasma-vacuum interface at the plasma boundary. They become global modes for $\Lambda \sim 1$. These features are illustrated in Fig. 5.

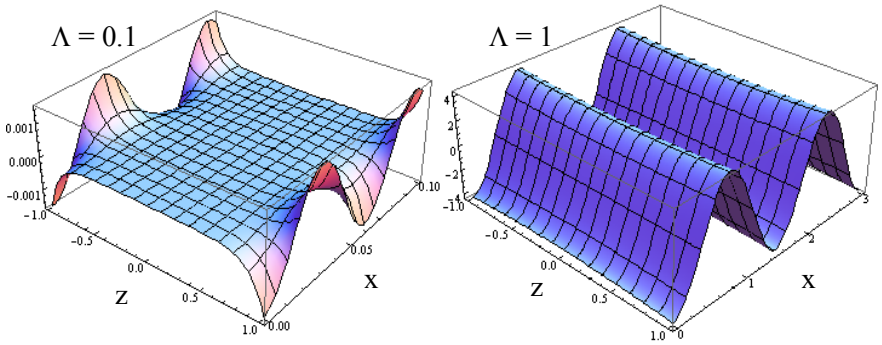

Fig. 5 Spatial structure of Re $E_z(x, z)$ for the sheath plasma wave (SPW) for the cases $\Lambda = 0.1$ (left) and $\Lambda = 1$ (right).

B. SW field pattern in the metal wall limit $\Lambda = 0$

Some useful insights can be gained by first examining the aperture problem in the metal wall $\Lambda = 0$ limit. For a delta-function source, this problem can be treated analytically in several limits. The expansion of the source

$$\sum_m C_m \cos k_{mz} z = \delta(z) \tag{13}$$

yields

$$C_m = \begin{cases} 1/2L & m = 0 \\ 1/L & m = 1, 2, \ldots \end{cases} \tag{14}$$

so the field solution is

$$E_z = \frac{1}{2L} e^{ik_{0x}x} + \sum_{m=1}^{\infty} \frac{1}{L} \cos k_{mz} z \; e^{ik_{mx}x}. \tag{15}$$

First considering b >> 1, Eq. (12) gives $k_{mx}^2\delta_e^2 \to -1$ which gives k_m independent of m, so the series can be re-summed and

$$E_z = \delta(z)\, e^{-x/\delta_e} \tag{16}$$

The field solution is a decaying "finger" into the plasma. However the solution is valid for $\eta^2 << b^2$ implying $n_z^2 << \varepsilon_\perp$, so that the "fingers" have long scale lengths in z >> c/ω. This is the electromagnetic limit. The voltage drop $\int dz\, E_z$ occurs in the plasma, and the structure does not reach the sheaths. At large x >> δ_e the voltage drop goes to zero. Note that $\int dz\, E_z$ along a field line (joining the two walls) is not conserved as a function of x because of enclosed electromagnetic flux.

Next considering b << 1, Eq. (12) with $\eta_m = m\pi$ gives $k_{mx} = im\pi/h$ for m ≠ 0, where h ≡ $b\delta_e$ while $k_{x0} = i/\delta_e$. Also, the definition of η gives $k_{zm} = m\pi/L$. The resulting geometric series is also summable and yields

$$2LE_z = e^{-x/\delta_e} - 2 + \frac{1}{1-e^{i\pi z/L-\pi x/h}} + \frac{1}{1-e^{-i\pi z/L-\pi x/h}} \tag{17}$$

The solution represents z-spreading and x-decay of the δ-function on a short radial scale ~ h ~ $(m_e/m_i)^{1/2}L$, followed by radial decay on the longer δ_e scale. The most persistent mode in x is given by the projection of the δ-function onto the lowest k_z mode, and this is the $k_z = 0$ mode for the conducting wall case. This small b case shows that rf fields get to the wall. Consequently the metal wall BCs are not necessarily self-consistent, because the implied sheath voltages and hence Λ are not necessarily negligible. We will return to this point in Sec. III.

C. SW field pattern for general Λ

The general Λ case must be treated numerically, so for better convergence of the sums we replace the δ-function source at x = 0 with a finite-width Gaussian

$$S(z) \equiv E_z(x=0,z) = \frac{V_0}{(2\pi)^{1/2}a}\exp\left(-\frac{z^2}{2a^2}\right) \tag{18}$$

For a << L, the normalization implies a launched voltage at the aperture of

$$V = \int_{-L}^{L} dz\, E_z(x=0) = V_0 \tag{19}$$

This source is expanded in terms of the eigenfunctions (see Appendix B).

From the preceding discussion, the problem with general Λ is of most interest for $b < 1$, so that the fields "see" the wall and the sheath BC. In the "dense" plasma limit, the condition $b < 1$ implies the estimate $L < \delta_i$ where $\delta_i = c/\omega_{pi}$ is the ion skin depth.

Before examining the numerical solutions, it is interesting to consider the analytical solution of the global dispersion relation Eq. (9) for $b << 1$ and $\Lambda > 1$. Expanding Eq. (9) in the limit of small η, we find that in this case the imaginary root or SPW approaches

$$\eta = ib\left(\frac{\Lambda}{\Lambda - 1}\right)^{1/2} \tag{20}$$

Further, considering the sub-limit $\Lambda \to \infty$ we obtain $\eta^2 + b^2 = 0$ or $n_z^2 = \varepsilon_\perp$, i.e.

$$k_z^2 v_a^2 = \frac{\omega^2}{1 - (\omega/\Omega_i)^2} \tag{21}$$

This allows the SPW to be associated with the Alfvén resonance. Alfvén resonance normally occurs for real k_z and $\omega < \Omega_i$. Here, Eq. (21) is satisfied for $\omega > \Omega_i$ but imaginary k_z. Imaginary k_z, i.e. modes with $E_z \sim \cosh(k_z z)$, are allowed by the sheath BC.

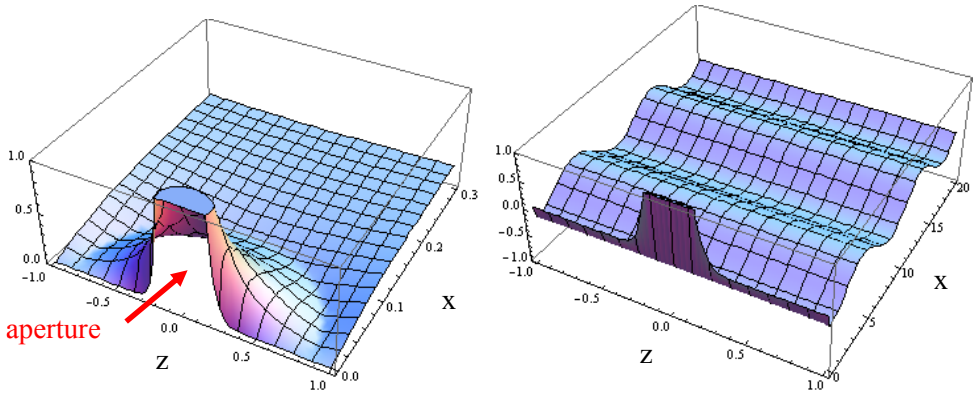

Fig. 6 Field pattern and emergence of the SPW for specified Λ. (left): $|E_z(x, z)|$ for $b = 0.1$ and $\Lambda = 3$. The scale in z is normalized to L and the scale in $x = (0, 0.3)$ is normalized to δ_e. (right): Re $E_z(x, z)$ for the same case, but with x shown over the range $x = (0, 20)$ to show the propagating SPW.

Turning to the numerical results, from Fig. 6, the short scales in z are seen to spread in z but evanesce rapidity in x, on a scale $x \sim h \sim (m_e/m_i)^{1/2}L$. Long scale structures in z act on the $x \sim \delta_e$ scale and behave differently. In particular there is coupling to the SPW eigenfunction as shown on the lower part of the figure over a longer range in x. It is significant that these fields

persist asymptotically in x. There is no radial evanescence of the SPW, rather it is a radially propagating mode. In more realistic geometry we would expect this mode to follow the sheath boundary of a limiter radially into the plasma, until the limiter terminates.

The rf field strength at the wall, and the resulting rf sheath voltage are of interest. The sheath voltage is determined by matching the normal component of $\varepsilon\cdot\mathbf{E}$ on the plasma side of the interface to the normal component of **E** in the sheath (vacuum layer). Since **E** in the sheath layer is constant in the thin sheath approximation, the sheath voltage is given by

$$V_{sh} = \Delta\varepsilon_{||}E_z(z=L) \tag{22}$$

A substantial fraction of the launched voltage ends up on the sheaths for b << 1, as illustrated in Fig. 7. The propagating SPW has both plasma voltage and sheath voltage oscillations; here the absolute value is plotted. The total voltage $V_{sh}+V_{pl}$ is not conserved as a function of x because of electromagnetic effects, as discussed after Eq. (16). V_{sh} is about 70% of V_0 for the parameters of the figure: b = 0.1, a = 0.1, Λ = 3. Note again that V_{sh} asymptotes to a constant value as $x \to \infty$.

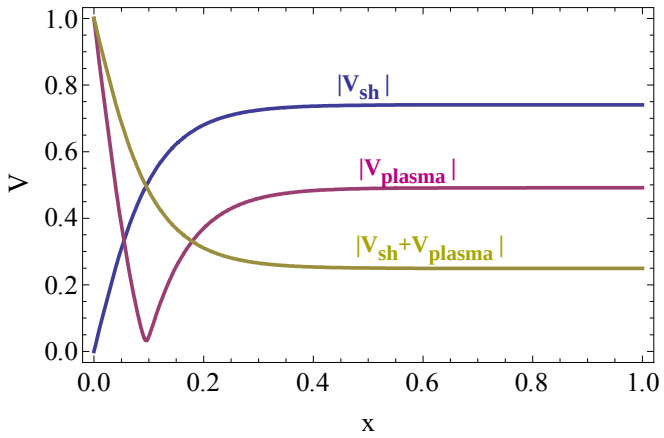

Fig. 7 Voltages $|V_{sh}|$, $|V_{pl}|$ and $|V_{sh}+V_{pl}|$ vs. x for the same parameters as Fig. 6. All voltages are normalized to the launched voltage V_0.

III. Self-consistent rf sheaths

The solutions of the preceding section, for specified Λ, are not in general self-consistent because the sheath width Δ should be determined from the sheath voltage and the Child-Langmuir law [36,37]

$$\Delta = \lambda_{de}\left(\left|\frac{\alpha e V_{sh}}{T}\right| + \alpha_{th}\right)^{3/4} \tag{23}$$

where λ_{de} is the electron Debye length, V_{sh} is obtained from Eq. (22), and α is an order unity factor (nominally $\alpha \sim 0.6$) which describes the rectification of rf to dc voltages. Eq. (23), which assumes a rectified voltage of order αV_{sh}, is strictly valid in the limit $eV_{sh}/T >> 1$, but has been Pade-approximated, using $\alpha_{th} \sim 1 - 3$, to yield $\Delta \sim \lambda_{de}$ for the case $eV_{sh}/T << 1$ where the sheath is just the thermal (Bohm) sheath. (See the appendix of Ref. [38] for a Bessel function model which gives a more accurate interpolation between the strong rf driven regime and the thermal sheath.)

The Child-Langmuir law may be written in the form

$$V_{sh} + V_{th} = \left(\frac{\Lambda}{\Lambda_0}\right)^{4/3} \equiv V_{CL} \tag{24}$$

where all voltages are normalized to the source voltage V_0, $V_{th} = \alpha_{th}T/(\alpha e V_0)$ is the (normalized thermal (Bohm) sheath voltage, and a reference value of Λ has been introduced, viz.

$$\Lambda_0 = -\frac{\lambda_{de}\varepsilon_{||}}{L}\left|\frac{\alpha e V_0}{T}\right|^{3/4} \tag{25}$$

Then, for a given Λ_0 we can determine the self-consistent Λ satisfying Eq. (24), using Eqs. (11), (22) and the field solution to determine $V_{sh}(\Lambda)$.

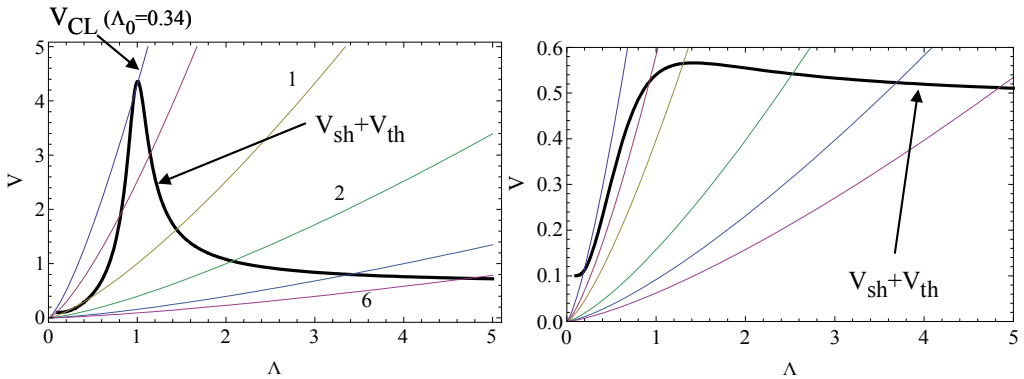

Fig. 8 Graphical solution of Eq. (24) for two values of b. $V_{sh} + V_{th}$ (thick black) and V_{CL} (colored, for various Λ_0) Left panel: b = 0.1 and Λ_0 = 0.34, 0.5, 1, 2, 4, 6. Right panel: b = 0.8 and Λ_0 = 1, 1.5, 2, 4, 6, 8. For these cases V_{th} = 0.1 and *a* = 0.1.

It is instructive to first examine the solution graphically. The left- and right-hand sides of Eq. (24) are illustrated in Fig. 8 for two cases, b = 0.1 and b = 0.8. Note that $V_{sh}(\Lambda)$ displays a resonant structure about $\Lambda \sim 1$ for the b = 0.1 case. $\Lambda = 1$ is the sheath-plasma resonance [33,34] and corresponds physically to a series resonance between the inductance of plasma ($\varepsilon_{||} < 0$ which implies a return current) and the sheath capacitance (from the vacuum gap of width Δ). For $b << 1$ this resonant structure results in multiple roots of Eq. (24) over a certain range of Λ_0, reminiscent of what was found in the FW $\rightarrow$ SW "scattering" problem. [20] At moderate $b \sim 1$ the vestige of the sheath-plasma resonance is very broad, and only single roots are possible.

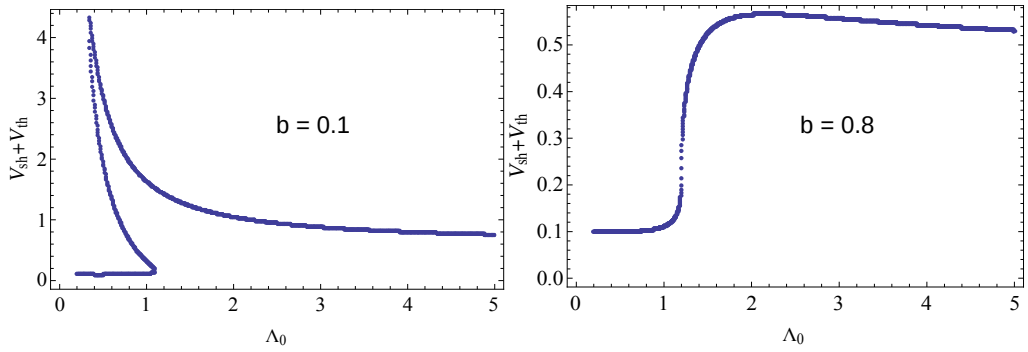

Fig. 9 Self-consistent sheath voltage at large x from the SPW. All voltages are normalized to the source voltage V_0. The normalized thermal (Bohm) sheath voltage is $V_{th} = 0.1$.

Using a root-finder to obtain the self-consistent value of Λ one can then determine the self-consistent sheath voltage as a function of the input parameter Λ_0. Results are shown in Fig. 9 for the same two cases, again normalizing all voltages to V_0. Strong amplification of V_0 is possible for $b << 1$ near SPW resonance at $\Lambda \sim 1$. For moderate b, the root makes a step-like transition from the thermal sheath voltage to the rf-dominated voltage. For still larger b (not shown), comparing with the $b \sim 1$ case, the transition occurs for slightly larger Λ_0 and the large Λ_0 plateau for V_{sh} is smaller. Recall that for $b >> 1$, there is no interaction with the wall.

IV. Summary and conclusions

Noting that $b \sim \delta_i/L$ (well into the dense plasma regime, and for $\omega > \Omega_i$) the present results show that there is significant transfer of SW voltage launched at the aperture to the sheaths at the wall if (i) the wall is at a parallel distance from the aperture that is less than δ_i, and (ii) the launched voltage is sufficiently strong, i.e. roughly $\Lambda_0 > 1$.

In an rf power scan (i.e. a Λ_0 scan), for a given b there is a critical value of $\Lambda_0 = \Lambda_c$ below which there is negligible sheath interaction (i.e. just the thermal sheaths are present).

Above Λ_c, there is an abrupt transition to a state with strong sheath interaction and significant coupling of energy into a propagating SPW, that is related to both the Alfvén resonance electromagnetically and the sheath-plasma resonance (in the electrostatic limit). This propagating wave carries the sheath voltages and the SW fields long distances compared with δ_e or $(m_e/m_i)^{1/2}L$, which are the radial evanescence scales in the absence of the SPW. Near Λ_c and for $b << 1$, i.e. close by walls or limiters, strong *amplification* of the launched V_0 is possible due to the sheath-plasma resonance. Finally we note that $b << 1$ is possible when $\varepsilon_\perp \approx 0$, i.e. near lower-hybrid resonance.

We have already noted a similarity of the present results with those of Ref. 20 in terms of the multiple roots and the possibility of resonant enhancement of the sheath voltage by the SPW. We can also compare with Fig. 2 which summarizes the results of the previous study on interaction of resonance cones with the wall sheaths, i.e. the aperture problem in tenuous plasmas. [31] Although the form of the computed $V_{sh}(\Lambda_0)$ curves are different in Figs. 2 and 9, in both cases there is an effective threshold value of Λ_0, or rf power, beyond which strong sheath interactions giving $V_{sh} \sim V_0 >> V_{th}$ are expected. There are some important differences between the two situations, however. In the dense plasma case Λ_0 is defined by Eq. (25) and the parallel scale length which enters is $L = L_{||}$, the distance from the source aperture to the wall. In the tenuous plasma, resonance cone case, Λ_0 is defined in Fig. 2, and the parallel scale length which enters is $a_{||}$, the parallel scale length of the resonance cone. (Because ideal resonance cones propagate without dispersion or spreading, the distance from the source to the wall does not enter.)

Finally, it is worth reiterating that the dense plasma case produces negligible sheath interaction if the nearest limiters or walls are further away along B than a critical length, typically δ_i. This means that in the remote limiter case, $L_{||} >> \delta_i$, strong sheath interactions are only possible in the tenuous plasma limit, $\omega > \omega_{lh}$.

Acknowledgments

We thank the RF SciDAC team for many useful discussions. This work was supported by USDOE grants DE-FG02-97ER54392 and DE-FC02-05ER54823 (the RF SciDAC project); however, such support does not constitute an endorsement by the DOE of the views expressed herein.

Appendix A: Slow wave eigenvector

Starting with the cold fluid dielectric tensor and taking the slow wave ordering $\varepsilon_{||} \sim n_{\perp}^2 >> \varepsilon_{\perp}, n_{||}^2$ the reduced slow wave equations for plane waves ~ exp(i**k**·**x**) are

$$\begin{pmatrix} \varepsilon_{\perp} - n_z^2 & n_x n_z \\ n_x n_z & \varepsilon_{||} - n_x^2 \end{pmatrix} \begin{pmatrix} E_x \\ E_z \end{pmatrix} = 0 \tag{A1}$$

where the notations are as in the main text: wave-vector $\mathbf{k} = k_x\mathbf{e}_x + k_z\mathbf{e}_z$ and z is along **B**. The determinant of the matrix gives the SW dispersion relation

$$n_x^2\varepsilon_{\perp} + n_z^2\varepsilon_{||} = \varepsilon_{\perp}\varepsilon_{||}. \tag{A2}$$

Instead of plane waves, we need the solution for sin and cos functions in a box. To determine the eigenvector for the even modes $E_z(z)$ we write the first row from Eq. (A1) in differential form as

$$\left(\varepsilon_{\perp} + \frac{c^2}{\omega^2}\frac{\partial^2}{\partial z^2}\right)E_x - i\frac{c}{\omega}n_x\frac{\partial E_z}{\partial z} = 0. \tag{A3}$$

Then taking $E_z \sim \cos(k_z z)$ yields Eq. (8) of the main text.

Appendix B: Complete set conjecture for finite Λ

A subtle question that arises is the completeness of the set of eigenmodes for general values of Λ. For Λ = 0 we know that the set of modes $\psi_m = \cos(k_{mz}z)$ with $\eta_m = m\pi$ (m = 0, 1, 2, …) form a complete set. Thus it might at first appear that the extra SPW root that emerges from η = ∞ at finite Λ is not needed. Similar remarks apply approaching finite Λ from the Λ = ∞ limit.

To address this question, consider the projection of the localized source given by Eq. (18) onto the full set of eigenfunctions including the SPW.

$$S(z) = \sum_{m=1}^{\infty} C_m\psi_m(z) + C_{\xi}\psi_{\xi}(z) \equiv \sum_{j=0}^{\infty} C_j\psi_j(z). \tag{B1}$$

The modes $\psi_m(z) = \cos(\eta_m z/L)$, and $\psi_\xi(z) = \cosh(\xi z/L)$ with $\xi = i\eta$ and η determined by Eq. (9), are in general not orthogonal. Thus, to determine the C_j in the expansion, one must solve a matrix equation obtained by projecting Eq. (A1) onto the modes

$$\sum_j^\infty \left\langle \psi_n(z)\psi_j(z) \right\rangle C_j = \left\langle \psi_n(z) S(z) \right\rangle . \tag{B2}$$

where

$$\langle ... \rangle = \frac{1}{L}\int_0^L dz\,(...) . \tag{B3}$$

Numerically, we find that the full matrix $\left\langle \psi_n(z)\psi_j(z) \right\rangle$ (including the SPW mode) is always invertible for the all the cases checked, and a well-conditioned and unique result for C_j is obtained. This is the basis for our conjecture that the ψ_j form a complete set.

The SPW expansion coefficient C_ξ for the Gaussian source is shown in Fig. 10 as a function of Λ. For $\Lambda = 0$ and $\Lambda = \infty$ we find $C_\xi = 0$, so while the SPW exists formally in these cases, there is no coupling to it, and the remaining ψ_m functions are sufficient to yield a complete set in these limits. For finite, non-zero Λ, however, the SPW eigenmode is essential to the decomposition. Note the SPW resonance near $\Lambda = 1$.

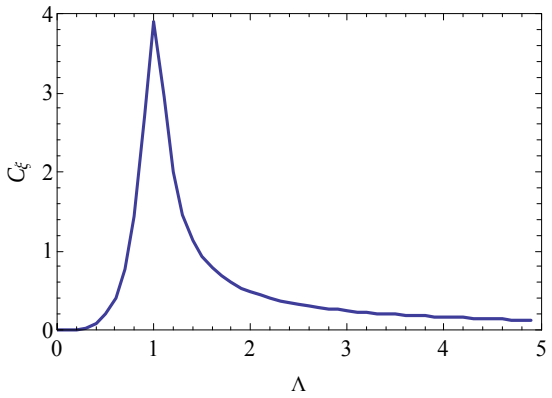

Fig. B1 Coefficient C_ξ of the SPW obtained by projecting the Gaussian source onto the SPW eigenmode for various Λ.

References

1 Noterdaeme J-M and Van Oost G 1993 *Plasma Phys. Control. Fusion* **35** 1481

2 Myra J R, D'Ippolito D A, Russell D A, Berry L A, Jaeger E F and Carter M D 2006 *Nucl. Fusion* **46** S455

3 Shimada M, Campbell D J, Mukhovatov V, Fujiwara M *et al*. 2007 *Nucl. Fusion* **47** S1

4 Butler H S and Kino G S 1963 *Phys. Fluids* **6** 1346

5 Perkins F W 1989 *Nucl. Fusion* **29** 583

6 Chodura R and Neuhauser J, *Proc. 16th European Conf. on Controlled Fusion and Plasma Heating*, Venice, Italy (European Physical Society, Petit-Lancy, 1989) vol 13B, part III, p 1089
Chodura R 1990 *Fusion Eng. Des.* **12** 111

7 Van Nieuwenhove R and Van Oost G 1989 *J. Nucl. Mater.* **162–164** 288

8 Myra J R, D'Ippolito D A, and Gerver M J 1990 *Nucl. Fusion* **30** 845

9 D'Ippolito D A, Myra J R, Bures M, and Jacquinot J 1991 *Plasma Phys. Controlled Fusion* **33** 607

10 Brambilla M *et al*, *Proc. 13th Int. Conf. on Plasma Physics and Controlled Nuclear Fusion Research 1990* (Washington DC, USA, 1991) (Vienna: IAEA) vol 1, p 723

11 Van Nieuwenhove R and Van Oost G 1992 *Plasma Phys. Control. Fusion* **34** 525

12 Myra J R, D'Ippolito D A and Bures M 1994 *Phys. Plasmas* **1** 2890

13 D'Ippolito D A and Myra J R 2006 *Phys. Plasmas* **13** 102508

14 Jaeger E F, Berry L A, Tolliver J S and Batchelor D B 1995 *Phys. Plasmas* **2** 2597

15 Carter M D, Godyak V, Hoffman D, Lee W S, Buchberger D and Ryan P M 2006 *J. Appl. Phys.* **100** 073305

16 Hosea J, Bell R E, LeBlanc B P, Phillips C K *et al*. 2008 *Phys. Plasmas* **15** 056104

17 Lee J H, Peebles W A, Jaeger E F, Doyle E J *et al*. 1998 *Phys. Rev. Lett.* **80** 2330

18 Hellsten T, Laxåback M, Bergkvist T, Johnson T *et al*. 2005 *Nucl. Fusion* **45** 706

19 Hellsten T and Laxåback M 2005 *Phys. Plasmas* **12** 032505

20 D'Ippolito D A, Myra J R, Jaeger E F and Berry L A 2008 *Phys. Plasmas* **15** 102501

21 D'Ippolito D A and Myra J R 2009 *Phys. Plasmas* **16** 022506

22 D'Ippolito D A and Myra J R, *Proc. 18th Topical Conf. on Radio Frequency Power in Plasmas*, (AIP, New York, 2009), p xx (in press)

23 Colas L, Heuraux S, Brémond S and Bosia G 2005 *Nucl. Fusion* **45** 767

24 Maggiora R, Vecchi G, Lancellotti V and Kyrytsya V 2004 *Nucl. Fusion* **44** 846

25 Van Compernolle B, Maggiora R, Vecchi G, Milanesio D and Koch R 2008 *Europhysics Conference Abstracts*, vol 32F:P-2.105 [presented at the 35th EPS Conference on Plasma Physics, Hersonissos, Crete (Greece) - 9/13 June 2008]

26 Bobkov V et al., Proc. 22nd IAEA Fusion Energy Conference, Geneva, Switzerland, October 13 - 18, 2008, (IAEA, Vienna, 2009) paper IAEA-CN-165/EX/P6-31.
Bobkov V et al., *Proc. 18th Topical Conference on Radio Frequency Power in Plasmas* (AIP, New York, 2009) p xx (in press).

27 Hutchinson I H *et al.* 1994 *Phys. Plasmas* **1** 1511

28 Lipschultz B, Pappas D A, LaBombard B, Rice J E, Smith D and Wukitch S J 2001 *Nucl. Fusion* **41** 585

29 Wukitch S J *et al*., *Proc. 21st IAEA Fusion Energy Conference*, Chengdu, 2006 (IAEA, Vienna, 2007) paper IAEA-CN-149-FT/1-6

30 Kohno H, Myra J R and D'Ippolito D A 2009 *Bull. APS* **xx** xx (in press)

31 Myra J R and D'Ippolito D A 2008 *Phys. Rev. Lett.* **101** 195004

32 Myra J R and D'Ippolito D A, *Proc. 18th Topical Conference on Radio Frequency Power in Plasmas* (AIP, New York, 2009) p xx (in press)

33 Myra J R, D'Ippolito D A, Forslund D W and Brackbill J U 1991 *Phys. Rev. Lett.* **66** 1173 and refs. therein

34 Stenzel R L 1988 *Phys. Rev. Lett.* **60** 704
Stenzel R L 1989 *Phys Fluids B* **1** 2273
and refs. therein

35 Bekefi G, *Radiation Processes in Plasmas* (Wiley, New York, 1966) chap 5

36 Child C D 1911 *Phys. Rev.* **32** 492
Langmuir I 1923 *Phys. Rev.* **21** 419

37 Chen F F, *Introduction to Plasma Physics* (Plenum, New York, 1974)

38 D'Ippolito D A and Myra J R 1996 *Phys. Plasmas* **3** 420